Available online at www.sciencedirect.com
SCIENCE DIRECT®
Journal of Solid State Chemistry 178 (2005) 1533–1538
JOURNAL OF SOLID STATE CHEMISTRY
www.elsevier.com/locate/jssc

Structural study of tungstate fluorophosphate glasses by Raman and X-ray absorption spectroscopy

Gaël Poirier[a,*], Younes Messaddeq[a], Sidney J.L. Ribeiro[a], Marcel Poulain[b]

[a]*Instituto de Química, UNESP, CP 355, CEP 14801-970, Araraquara, SP, Brazil*
[b]*Laboratoire des Matériaux Photoniques, Bât 10B, Campus de Beaulieu, Université de Rennes I, Rennes, France*

Received 8 September 2004; received in revised form 27 October 2004; accepted 28 October 2004
Available online 25 March 2005

Abstract

Transparent glasses were synthesized in the $NaPO_3$–BaF_2–WO_3 ternary system and several structural characterizations were performed by X-ray absorption spectroscopy (XANES) at the tungsten L_I and L_{III} absorption edges and by Raman spectroscopy. Special attention was paid to the coordination state of tungsten atoms in the vitreous network.

XANES investigations showed that tungsten atoms are only six-fold coordinated (octahedra WO_6) and that these glasses are free of tungstate tetrahedra (WO_4).

In addition, Raman spectroscopy allowed to identify a break in the linear phosphate chains as the amount of WO_3 increases and the formation of P–O–W bonds in the vitreous network indicating the modifier behavior of WO_6 octahedra in the glass network. Based on XANES data, we suggested a new attribution of several Raman absorption bands which allowed to identify the presence of $W–O^-$ and $W{=}O$ terminal bonds and a progressive apparition of W–O–W bridging bonds for the most WO_3 concentrated samples ($\geqslant 30\%$ molar) due to the formation of WO_6 clusters.
© 2004 Elsevier Inc. All rights reserved.

Keywords: Tungsten; Phosphate glasses; XANES; Raman; WO_6 cluster

1. Introduction

Fluorophosphate glasses were intensively investigated because of their well known particular interesting properties such as larger thermal expansion coefficient, smaller liquidus viscosity and softening temperatures than silicate glasses as well as high UV transmission which can make them suitable as laser hosts [1–5]. Another interesting feature of these glasses is their ability to incorporate large amounts of transition metal, alkali and rare earth oxides without reduction of glass forming ability.

Tungsten oxide containing glasses are of great interest because they can exhibit any unusual electrochromic or photosensitive properties related to the ability of tungsten atoms to adopt various oxidation states (W^{6+}, W^{5+} or W^{4+}). Moreover, it was already assumed that tungsten oxide units participate in the glass network [6–9] and can improve considerably the chemical durability and thermal stability against devitrification [10–12].

In this way, tungstate fluorophosphate glasses are promising materials because of their particular chemical, physical and optical properties. We reported elsewhere their optical properties such as upconversion phenomena when doped with Tm^{3+} or two photon nonlinear absorption for the most WO_3 concentrated glasses [13,14]. However, the structure of WO_3-based glasses and especially the coordination state of tungsten atoms is not well understood. Indeed, a majority of authors agree that tungsten oxide units are present in the glass network as WO_4 tetrahedra and WO_6 octahedra whereas a few of them suggest that only six-fold

*Corresponding author. Fax: +55 16 3222 5987.
E-mail address: gael@posgrad.iq.unesp.br (G. Poirier).

0022-4596/$ - see front matter © 2004 Elsevier Inc. All rights reserved.
doi:10.1016/j.jssc.2004.10.032

coordinated tungsten atoms are present in the glass [15–18].

The objective of the present work is to investigate the structure of glasses obtained in the $NaPO_3$–BaF_2–WO_3 system [13] by XANES spectroscopy at the tungsten L_I and L_{III} absorption edges and by Raman spectroscopy. In particular, the aim of this structural investigation is to determine the coordination state of tungsten atoms in these tungstate fluorophosphate glasses.

2. Experimental procedure

2.1. Sample preparation

These glasses were synthesized by conventional method. Powdered starting materials such as

- tungsten oxide WO_3 from Alpha (99.8% pure),
- sodium polyphosphate $NaPO_3$ from Acros (99 + % pure),
- and barium fluoride BaF_2 from Aldrich (99.8% pure),

were mixed and heated at 400°C for 1 h to remove water and adsorbed gas. Then, the batch was melted at a temperature ranging from 800 to 1100 °C, depending on WO_3 content. Liquid was kept at this temperature for 15–75 mn to ensure homogenization and fining. Finally the melt was cooled in a brass mold preheated at the transition temperature T_g. Annealing was implemented at this temperature for several hours in order to minimize mechanical stress resulting from thermal gradients upon cooling. The amorphous state of each sample was checked by X-ray diffraction. Glass samples were synthesized in the (80–0.8x) $NaPO_3$—(20–0.2x) BaF_2–xWO_3 ternary system. The molar concentration, glass transition temperature and color are presented in Table 1 for each sample.

2.2. Physical measurements

Tungsten L_I (12,100 eV) and L_{III} (10,207 eV) X-ray absorption near edge structure (XANES) measurements were performed on the XAS beam line at LNLS (Campinas–Brazil) working with an electron energy of 1.37 GeV and a maximum electron current of 250 mA. A double crystal Si (1 1 1) monochromator used to obtain the monochromatic X-ray incident beam was first calibrated using the Zn K absorption edge as reference (9659 eV). The energy steps and counting times were adjusted to improve the resolution and are presented in Table 2.

Table 1
Molar concentrations, glass transition temperature values and colors of glass samples

Sample	$NaPO_3$	BaF_2	WO_3	T_g	Color
NBW0	80	20	0	240	Colorless
NBW10	72	18	10	280	Colorless
NBW20	64	16	20	320	Colorless
NBW30	56	14	30	370	Colorless
NBW40	48	12	40	418	Yellow
NBW50	40	10	50	465	Deep blue
NBW60	32	8	60	524	Blue

Table 2
Energy steps and counting times for XANES measurements

Absorption edge	Energy (eV)	Step (eV)	Counting time (s)
L_I	12070–12090	2	3
	12090–12140	1	3
	12140–12200	2	3
L_{III}	10150–10190	2	3
	10190–10230	1	3
	10230–10280	2	3

Data were collected at room temperature in transmission mode using ionization chambers filled with helium. Samples were prepared by grinding and sieving glasses to obtain fine powders with regular grain size of 20 μm. The mass powder necessary for the measurements has been previously computed to avoid saturation effects and to optimize the signal to noise ratio. The powders were then dispersed in ethanol and deposited in a microporous membrane to obtain sample deposits.

All the spectra were treated with the same procedure. The absorption background was subtracted using a linear extrapolation, E_0 was determined at the inflection point of the absorption edge and the spectra then normalized by taking an energy point around 50 eV above the edge.

Raman scattering spectra were recorded at room temperature in the wave number range from 1300 to 200 cm^{-1} using a Renishaw micro-Raman spectrometer with a single monochromator and a filter. The excitation was provided by a He–Ne laser at 633 nm and the monochromator was operating with a resolution of about 6 cm^{-1}. All measurements were carried out on bulk vitreous samples.

3. Results

3.1. Tungsten L_I edge XANES spectroscopy

Normalized XANES spectra registered at the W L_I absorption edge (12,100 eV) are presented in Fig. 1a for crystalline compounds and vitreous samples. The crystalline compounds used as references are:

- Sodium tungstate Na_2WO_4 from Aldrich (99 + %) is a cubic phase with space group $Fd3m$ [19]. In this

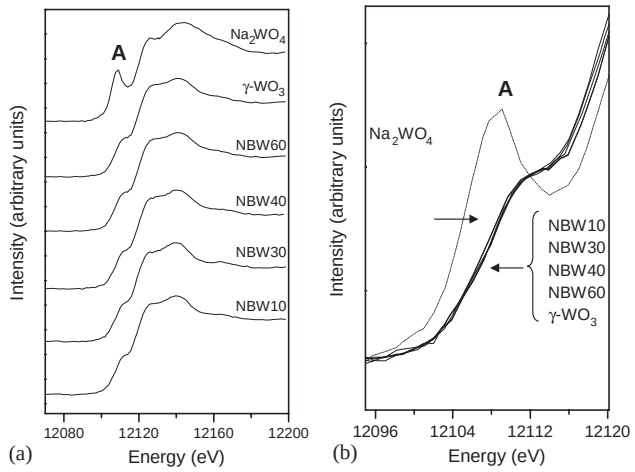

Fig. 1. Normalized W L_I edge XANES spectra of crystallized references γ-WO_3 and Na_2WO_4 and of vitreous samples.

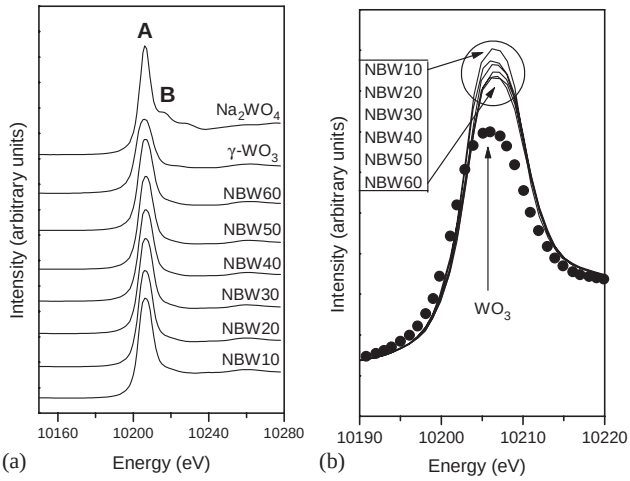

Fig. 2. Normalized W L_{III} edge XANES spectra of crystallized references γ-WO_3 and Na_2WO_4 and of vitreous samples.

compound, the tungsten atom is in a regular tetrahedral coordinance WO_4.

- Tungsten oxide WO_3 from Alpha (99.8%) is a monoclinic phase with space group $P2_1/n$ [20]. In this compound, the tungsten atom is in a distorted octahedral coordinance WO_6.

Vitreous samples were synthesized in the (80–0.8x) $NaPO_3$—(20–0.2x) BaF_2—xWO_3 system with $x = 10$, 30, 40 and 60.

The intensity of the pre-edge feature labeled A observed for all the references and samples depends of the site symmetry of the transition metal ion. In fact, this pre-edge absorption is due to a $2s(W) \rightarrow 5d(W) + 2p(O)$ electronic transition which is dipole forbidden in the case of regular octahedra (inversion center) but allowed for distorted octahedra and tetrahedra [21–23]. The intensity of the pre-edge feature A appears to be the largest for sodium tungstate Na_2WO_4 where W is tetrahedral but is very weak in the case of monoclinic γ-WO_3 where W is in a distorted octahedral configuration. Fig. 1a shows that the XANES spectra of the vitreous samples and of γ-WO_3 are very similar. A more detailed view is proposed in Fig. 1b in the 10,190–10,220 eV energy range. The intensity of the pre-edge feature A is very similar for vitreous samples and γ-WO_3 but very different from Na_2WO_4 indicating that tungsten atoms forms only distorted octahedra (WO_6) for all the compositions and that these glasses are free of WO_4 tetrahedra. In addition, while the intensity of this pre-edge feature A is directly related to the degree of WO_6 distortion, we assumed that the distortion of tungstate octahedra in the vitreous samples is similar to that of γ-WO_3.

3.2. Tungsten L_{III} edge XANES spectroscopy

Fig. 2a shows the W L_{III} edge XANES spectra of any crystalline references (γ-WO_3 and Na_2WO_4) and of vitreous samples ($x = 10$, 20, 30, 40, 50, 60). These spectra differ by the amplitude of the "white line" resonance, labeled A, and the presence or not of a post-edge feature, labeled B after the absorption edge. The white line A is due to the electronic transition $2p_{3/2}(W) \rightarrow 5d(W) + 2p(O)$ [22,23] and its amplitude is directly related to the local density of d states, thus to the number of unoccupied 5d states. Consequently, the characteristics of the white line depend of the local environment around the tungsten atom. The decrease of intensity shows a modification of the distortion of WO_6 octahedra [23].

In Fig. 2b are represented the relative intensity of the white line for γ-WO_3 and each of the vitreous samples. We can note that the relative intensity of the white line decreases with increasing the amount of WO_3 and is progressively close to that of γ-WO_3 suggesting an increase of the WO_6 distortion with the WO_3 content.

The absence of a post-edge feature B in the glasses, as encountered in Na_2WO_4, provides the assumption that the tungsten atoms are only six-fold coordinated in our glasses.

3.3. Raman spectroscopy

The Raman scattering spectra for $NaPO_3$, γ-WO_3 and Na_2WO_4, used as references, are shown in Fig. 3.

Sodium polyphosphate $NaPO_3$ is built up of linear PO_4 chains, thus each tetrahedra possesses two bridging oxygen (P–O–P) and two terminal oxygen (P═O and P–O^-) which are equivalent by resonance. $NaPO_3$ Raman spectrum, shown in Fig. 3, presents two intense bands centered around 700 cm^{-1} and 1160 cm^{-1} assigned to symmetrical stretching vibrations of P–O–P linkages [24–27] and symmetrical stretching vibrations of terminal P–O bonds in Q^2 tetrahedra, respectively [28] and three weak bands centered around 330, 1010 and

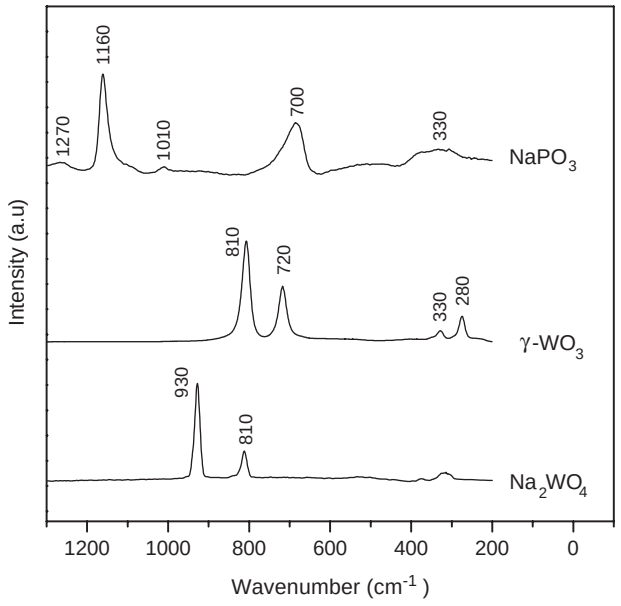

Fig. 3. Raman spectra of $NaPO_3$, octahedral γ-WO_3 and tetrahedral Na_2WO_4.

$1270\,cm^{-1}$ assigned to the bending vibrations of PO_4 tetrahedra, symmetric stretching vibrations of terminal P–O bonds in Q^1 tetrahedra and asymmetric stretching vibrations of terminal P–O bonds in Q^2 tetrahedra [29]. In sodium polyphosphate, Q^1 tetrahedra are located at the end of the linear chains of PO_4 entities.

Monoclinic tungsten oxide γ-WO_3, with $P2_1/n$ space group [30], is constituted of distorted WO_6 octahedra where all the corners are shared with another octahedron building up a tridimensional crystalline network. Consequently, γ-WO_3 does not possess any terminal W–O bonds ($W–O^-$ or $W{=}O$) but only W–O–W bridging bonds. Its Raman spectrum, shown in Fig. 3, presents two bands at 810 and $720\,cm^{-1}$ assigned to asymmetric and symmetric stretching vibrations of W–O–W linkages, respectively, and two weak shoulders at 330 and $280\,cm^{-1}$ assigned to bending vibrations of WO_6 octahedra [17].

Sodium tungstate Na_2WO_4 is built up with isolated WO_4^{2-} tetrahedra where all the W–O bonds are terminal (two $W{=}O$ and two $W–O^-$ bonds equivalent by resonance). Its spectrum shows two bands centered at 930 and $810\,cm^{-1}$. Several works attributed these Raman bands to stretching vibrations of W–O terminal bonds in WO_4 [31–33] based on the fact that they are present in the Raman spectra of crystalline tetrahedral references M_nWO_4 (M = Li, Na, Ca, etc.…) but not on the spectrum of γ-WO_3 (octahedral configuration). However, recent structural investigations were performed on $Li_2W_2O_7$ by Raman scattering [34] and apparently contradict these Raman bands attributions. In fact, this compound is built up with LiO_4 tetrahedra and very distorted WO_6 octahedra sharing their edges to form anionic $(W_2O_7)^{2-}$ chains. LiO_4 tetrahedra connect these chains by sharing their corners with WO_6 octahedra. Thus, this compound possesses bridging W–O–W bonds linking WO_6 octahedra in the plane, terminal W–O bonds between the WO_6 planes and all the tungsten atoms are six-fold coordinated. In fact, its Raman spectrum exhibits two bands at 810 and $720\,cm^{-1}$ due to W–O–W bridging bonds but also another one at $930\,cm^{-1}$ like for tetrahedral compounds. Consequently, the bands observed at 930 and $810\,cm^{-1}$ for Na_2WO_4 cannot be assigned to stretching vibrations of WO_4 units but are assumed to be due to asymmetric and symmetric stretching vibrations of terminal W–O bonds, respectively [17,35]. Sekiya et al. suggested that the position of these bands is independent of the tungsten coordination number and thus, does not allow to identify the tungsten environment [17].

Fig. 4 compares Raman spectra of the vitreous samples and of the crystalline references. Two bands centered at 1160 and $1010\,cm^{-1}$ decrease in intensity by increasing WO_3 content and disappear when the amount of WO_3 is higher than 30%. They are attributed to symmetric stretching vibrations of P–O terminal bonds

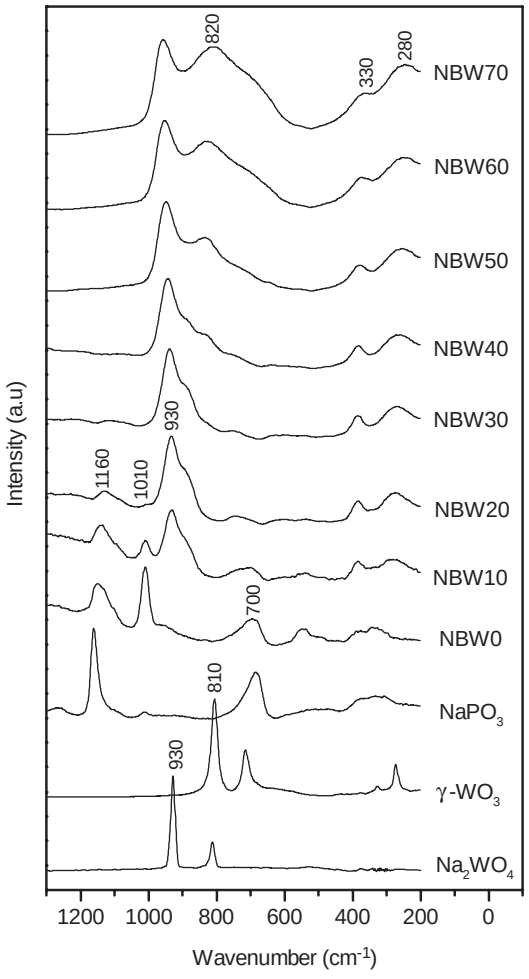

Fig. 4. Raman spectra of the vitreous samples and of the references.

($P–O^-$ or P=O) in Q^2 metaphosphate and Q^1 pyrophosphate tetrahedra, respectively. In addition, the band near 700 cm^{-1} due to symmetric stretching vibrations of P–O–P bridging bonds decreased in intensity and shifts to higher frequencies with WO_3 incorporation. These results suggest a progressive break of the linear phosphate chains by insertion of WO_6 octahedra between PO_4 tetrahedra and formation of P–O–W bridging bonds along these chains. The weak band at 530 cm^{-1} for NBW0 is characteristic of P–F terminal bonds [36].

The Raman bands observed at 330 and 280 cm^{-1} for crystalline WO_3 appear as a broad band centered at 270 cm^{-1} for WO_3 containing glasses and is attributed to bending vibrations of WO_6 octahedra. These results are in good agreement with XANES investigations which showed that the tungsten atoms are in an octahedral configuration. Another weak band at 370 cm^{-1} is probably due to bending vibrations of W–O terminal bonds in WO_6 octahedra [37].

In addition, an intense band is observed at 930 cm^{-1} for all the WO_3 containing samples and is attributed to stretching vibrations of terminal W–O bonds as explained before in the case of Na_2WO_4. The shoulder at 880 cm^{-1} together with this band is due stretching vibrations of P–O terminal bonds in PO_4 tetrahedra linked with WO_6.

Finally, two bands appear around 820 and 720 cm^{-1} for vitreous samples containing more than 30% molar in WO_3 and increases in intensity with increasing WO_3 content. These bands which are attributed to stretching vibrations of W–O–W bridging bonds indicate that WO_6 octahedra are progressively linked together for the most WO_3 concentrated samples.

4. Discussion

The coordination number of tungsten atoms in these glasses was pointed out by W L_I XANES spectroscopy. In fact, the main XANES feature registered for these glasses in Fig. 1 is the pre-peak A observed for Na_2WO_4 which directly depends on the tungsten coordination number. Its very low intensity in the L_I XANES spectra of the vitreous samples clearly demonstrates that the tungsten atoms are only six-fold coordinated forming distorted WO_6 octahedra. The difference of intensity of the white line in the L_{III} XANES spectra suggests a modification of the distortion of WO_6 octahedra in function of the amount of WO_3. Further extended X-ray absorption fine structure (EXAFS) measurements will be performed to prove this behavior. In addition, L_{III} XANES measurements consolidate the L_I XANES data by showing that these glasses do not contain any WO_4 tetrahedra.

Structural investigations performed by Raman scattering showed largest modifications in the vitreous network in function of the WO_3 content. In fact, incorporation of WO_3 in a 80 $NaPO_3$—20 BaF_2-based glass progressively breaks the linear phosphate chains and the WO_6 octahedra are incorporated in the glass network between the PO_4 tetrahedra resulting in the formation of P–O–W bonds and of Q^1 and Q^0 phosphate tetrahedra. In this case, the Q^n tetrahedra don't possess 3-n terminal oxygens but these atoms are partially bonded to tungsten atoms. The creation of P–O–W bonds is in accordance with the increase of T_g values (Table 1) with the amount of WO_3 because of an increase in the network connectivity. Thus, in these glasses the vitreous covalent network consists in mixed chains composed of PO_4 tetrahedra and WO_6 octahedra.

Based on XANES results, the band at 930 cm^{-1} in the Raman spectra of these glasses cannot be assigned to WO_4 tetrahedra, but is due to W–O terminal bonds in WO_6 octahedra. The feature at 820 cm^{-1}, due to W–O–W bridging bonds, appears only for the most WO_3 concentrated samples and suggests a progressive clustering of the WO_6 entities for samples containing more than 30% molar of WO_3. This clustering can explain the nonlinear optical properties of the high WO_3 concentrated samples reported elsewhere [14].

A great majority of the structural works published on WO_3 containing glasses proposed the presence of only WO_4 tetrahedra [15,32] or the existence of a mixed W coordination state made of WO_4 tetrahedra and WO_6 octahedra [6,31,33] but only a few papers report the existence of tungsten ions in octahedral coordination whatever the glass composition [17,18]. Any of these works concluded to the presence of WO_4 tetrahedra by the observation of this intense band around 930 cm^{-1} in the Raman spectra. This work showed that this Raman band cannot be related to WO_4 tetrahedra and that XANES spectroscopy can be a very powerful tool to provide informations on the local symmetry and coordination around the tungsten atom.

5. Conclusion

Structural investigations were performed on the $NaPO_3$–BaF_2–WO_3 system using two complementary techniques in order to understand the vitreous network evolution in function of the amount of WO_3. W L_I XANES spectroscopy proved that tungsten atoms are only present in an octahedral configuration WO_6 whatever the glass composition whereas XANES measurements at the W L_{III} edge suggested a progressive modification of the WO_6 distortion in function of the WO_3 content.

Raman scattering pointed out that the introduction of WO_3 in the $NaPO_3$–BaF_2 binary system progressively depolymerizes the linear phosphate chains of PO_4 and results in the formation of P–O–W bonds which increase

the network connectivity. In addition, the apparition of W–O–W bonds for samples containing more than 30% molar in WO_3 enhances the hypothesis of the formation of clusters of WO_6 entities in these samples which can explain their non linear optical properties. Finally, it was shown that the well-known Raman band at $930\,cm^{-1}$ observed in several tungstate compounds is not necessarily due to WO_4 tetrahedra.

Acknowledgments

Financial support for this work by Programa de Nucleos de Excelência-PRONEX, FAPESP (Brazil) and Conseil Régional de Bretagne (France) are gratefully acknowledged.

References

[1] L. Bih, N. Allali, A. Yacoubi, A. Nadiri, D. Boudlich, M. Haddad, A. Levasseur, J. Phys. Chem. Glass. 40 (1999) 229.
[2] R.K. Brow, D.R. Tallant, J. Non-Cryst. Sol. 222 (1997) 396.
[3] S.W. Lee, J.H. Lee, J. Phys. Chem. Glasses 36 (1995) 127.
[4] Y.B. Peng, D.E. Day, Glass Technol. 32 (1991) 166.
[5] W. Matz, D. Stachel, E.A. Goremychkin, J. Non-Cryst. Sol. 101 (1988) 80.
[6] V. Dimitrov, M. Arnaudov, Y. Dimitriev, Monatshefte Chem. 115 (1984) 987.
[7] M. von Dirke, S. Mullar, M. Rager, J. Non-Cryst. Sol. 124 (1990) 265.
[8] G. Srinivasarao, N. Veeraiah, Phys. Status Solidi A 191 (2002) 370.
[9] P. Frobel, K. Barner, J. Non-Cryst. Sol. 88 (1986) 329.
[10] P. Subbalakshmi, N. Veeraiah, Phys. Chem. Glass. 42 (2001) 307.
[11] J.J. Rothermel, J. Am. Ceram. Soc. 32 (5) (1949) 153–162.
[12] O. Ya. Miroshnichenko, G.M. Khvedchenya, J. Appl. Chem. (USSR) 54 (1981) 563.
[13] G. Poirier, V.A. Jerez, C.B. de Araújo, Y. Messaddeq, S.J. L Ribeiro, M. Poulain, J. Appl. Phys. 93 (3) (2003) 1493–1497.
[14] G. Poirier, C.B. de Araújo, Y. Messaddeq, S.J. L Ribeiro, M. Poulain, J. Appl. Phys. 91 (12) (2002) 10221–10223.
[15] I. Shaltout, Y. Tang, R. Braunstein, E.E. Shaisha, J. Phys. Chem. Solids 57 (1996) 1223.
[16] V. Dimitrov, M. Arnaudov, Y. Dimitriev, Monatsh. Chem. 115 (1984) 987.
[17] T. Sekiya, N. Mochida, S. Ogawa, J. Non-Cryst. Sol. 176 (1994) 105.
[18] P. Charton, L. Gengembre, P. Armand, J. Sol. State. Chem. 168 (2002) 175–183.
[19] National Bureau of Standards, (US) Monograph 25 (1), 1962, p. 47.
[20] D. Grier, G. McCarthy, North Dakota State University, USA, ICDD Grant-in-Aid, 1991.
[21] A. Kuzmin, J. Purans, J. Phys. IV France 7 (1997) C2–971.
[22] J.A. Horsley, I.E. Wachs, J.M. Brown, G.H. Via, F.D. Hardcastle, J. Phys. Chem. 91 (1987) 4014.
[23] A. Balerna, E. Bernieri, E. Burattini, A. Kuzmin, A. Lusis, J. Purans, P. Cikmach, Nucl. Instrum. Methods Phys. Res. A 308 (1991) 240.
[24] R.J. Kirkpatrick, R.K. Brow, Sol. State Nucl. Magn. Reson. 5 (1995) 9–21.
[25] A. Kuzmin, J. Purans, J. Phys.: Condens. Matter 5 (1993) 9423.
[26] M. Tatsumisago, Y. Kowada, T. Minami, Phys.Chem.Glasses 29 (1988) 63.
[27] S.H. Morgan, R.H. Magruder, J.Am.Ceram.Soc. 73 (1990) 753.
[28] B.N. Nelson, G.J. Exarhos, J.Chem.Phys. 71 (1979) 2739.
[29] G.T. Stranford, R.A. Condrate, B.C. Cornilsen, J. Mol. Struct. 73 (1981) 231.
[30] B.O. Loopstra, P. Boldrini, Acta Crystallogr. 21 (1966) 158.
[31] M. Tatsumisago, Y. Kowada, T. Minami, H. Adachi, Phys. Chem. Glasses 35 (2) (1994) 89.
[32] I. Shaltout, Y.I. Tang, R. Braunstein, J. Phys. Chem. Sol. 56 (1) (1995) 141–150.
[33] B.V.R. Chowdari, P. Kumari, Mater. Res. Bull. 34 (2) (1999) 327.
[34] P. Charton, Ph.D. Thesis, Montpellier II University, France, 2002.
[35] M.S. Augsburger, J.C. Pedregosa, J. Phys. Chem. Solids 56 (8) (1995) 1081.
[36] R. Lebullenger, L.A.O. Nunes, A.C. Hernandes, J. Non-Cryst. Sol. 284 (2001) 55–60.
[37] J. Hanuza, L. Macalik, M. Maczka, E.T.G. Lutz, J.H. Van der Mass, J. Mol. Struct. 511–512 (1999) 85–106.